CONF-790606--9

THE CHANGE IN MECHANICAL PROPERTIES OF ANTRIM OIL SHALE ON RETORTING

MASTER

by S.P. Singh, W.A. Hockings, and
K. Kim, Michigan Technological Univ.

This paper was presented at the 20th U.S.Symposium on Rock Mechanics, held in Austin, Texas, June 4-6, 1979. The material is subject to correction by the author. Permission to copy is restricted to an abstract of not more than 300 words. Write: Dr. Ken Gray, U. of Texas at Austin, Petroleum Engineering Dept.

ABSTRACT

The decomposition of kerogen in oil shale and subsequent extraction of the decomposition products during the retorting process are known to alter the pore structure, resulting in changes in permeability, deformation and strength properties. Prediction of these changes is of fundamental importance in the design of *in-situ* retorting processes.

This paper summarizes a comprehensive laboratory investigation on the changes in mechanical properties of Antrim oil shale on retorting at 500°C. It was observed that kerogen plays an important role in the change of the properties on retorting. When subjected to heat, the degree of deformation, the extent of fracturing and the structural instability of the specimens appeared to be strongly dependent upon kerogen content. The values of elastic modulus, strength, and density decreased whereas maximum strain at failure increased on retorting.

Significant increases in permeability and porosity also resulted from retorting. The most pronounced increase was observed in the permeability in the direction parallel to bedding which exceeded in some cases as much as 3 orders of magnitude. Microscopic observations of pore structures provided a qualitative support to data obtained in measurements of porosity and permeability.

INTRODUCTION

It is estimated that 2.5 trillion barrels of shale oil are buried in the Antrim formation, an Upper Devonian organic rich, marine black shale which underlies the entire Michigan basin (1)(2). The Antrim shale varies from about 70 to 220 feet in thickness and the depth of the formation ranges from outcrop to 1600 feet in the center of the basin. The kerogen content of this black shale ranges from 6 to 10 gallons per ton. These factors require the development of a suitable true *in-situ* processing method.

References and illustrations at end of paper.

Decomposition of kerogen caused by retorting is known to result in significant changes in the structure and properties of oil shale. Little information is, however, available as to these changes despite their importance to the design of an *in-situ* retorting process (3)(5)(10).

The major difficulty in the development of *in-situ* retorting technology is that oil shale has low porosity and insignificant permeability. Therefore the design of an adequate *in-situ* retorting process necessitates the development of a suitable technique ensuring permeability generation and control. Proper understanding of and the solution to the porosity and permeability problem require basic knowledge of the influence of retorting on porosity and permeability of oil shale.

In the light of the aforementioned problems, it has been endeavored to make detailed laboratory investigations regarding the changes in the mechanical and physical properties of Antrim shale on retorting.

EXPERIMENTAL

Diamond cores obtained from Sanilac County, Michigan were tested in pre- and post-retorted conditions to study the following aspects:

(1) deformation and strength properties in uniaxial compression,
(2) porosity and permeability,
(3) pore structure by optical and scanning electron microscopy; and
(4) interrelationships among the above properties.

Cylindrical specimens of adequate size were prepared from the cores. The specimens were prepared in pairs with duplicate specimens having the same size and visual homogeneity. One specimen from each pair was roasted at 500°C in air. Heating and cooling was done at approximately 0.3°/sec to avoid excessive crack development due to thermal spalling. The specimens for uniaxial compression tests were roasted for 48 hours, whereas the specimens for porosity, permeability and microscopic work were roasted for five hours only. Percentage weight loss

for each specimen was determined at the end of the retorting procedure.

Uniaxial compression tests were conducted by using an ultra-stiff, computer-controlled testing system. Testing was started by initiating the preprogrammed computer program which provided a constant loading rate of approximately 0.7 MPa per second and graphical displays of stress, axial and circumferential strains, and time, etc. Descriptions of test methods can be found elsewhere (4).

Porosity and permeability were measured in parallel and perpendicular direction to the bedding plane. The diameter of the specimens was 1.35 cm and the length was about 2.5 cm. Permeability was measured by recording air flow through a specimen under a pressure gradient. The apparatus consists of a supply of dry air, mercury manometer, specimen holder and three capillary tubes of different cross-sectional areas. A schematic diagram of the permeability apparatus is shown in Figure 1. A pressure of 0.62 MPa was applied by compressed air on the rubber sleeve radially surrounding the specimen in the interior of the specimen holder to form a tight seal. One capillary of appropriate size was selected and the other two were closed. Dry air was forced through the core at a pressure differential of one atmosphere. The flow rate of the air passing through the specimen was determined by measuring the rate of movement of an oil bubble in the selected capillary tube. The permeability k was calculated by the equation

$$k = \frac{2 P_o Q_o \eta \, dL}{A(P_i^2 - P_o^2)}$$

where P_o and P_i are the outlet and the inlet absolute pressures, Q_o is the flow rate measured at the outlet end, η is the viscosity of air, dL is the length of the specimen in the direction of flow, and A is the cross-sectional area of the specimen.

In the present investigation the term porosity means apparent porosity, which is the ratio of the volume of the surface connected pores to the bulk volume. If D_g and D_a are the geometric and apparent densities, then

$$\text{apparent porosity} = \frac{D_a - D_g}{D_a}.$$

Geometric density was determined by finding the ratio between the weight and the external volume of the specimen. External volume was found by measuring the dimensions of the specimen with a caliper. Apparent density was calculated by the ratio between the specimen weight and the volume of the rock solids plus closed pores. This volume was measured with a gas pycnometer which employs a gas displacement technique (6).

RESULTS

During and after retorting, structural alterations were observed in specimens. In most of the kerogen-rich specimens, the development of fractures parallel to the bedding plane was observed at 230°-290°C. With further increases in temperature, existing fractures enlarged and additional ones were developed. The color of the specimens changed from light gray or black to light or dark brown. The specimens with less than four percent weight loss maintained structural integrity and experienced insignificant deformation, whereas the specimens with higher percentage weight loss exhibited significant structural deformation.

The results of uniaxial compression tests are presented in Table 1. The change of various parameters were plotted against % weight loss after retorting (Figures 2-4). The linear regression lines in each figure indicate that the changes which resulted from retorting become more pronounced with increasing % weight loss. The typical stress-strain curves given in Figure 5 also demonstrate clearly the effect of retorting on mechanical properties. Significant decreases in elastic modulus and compressive strength and increases in maximum strains are shown in this figure.

Porosity and permeability were measured in the specimens cored parallel and perpendicular to the bedding plane. The results for the retorted and unretorted specimens are given in Table 2. The unretorted specimens with inclusions of calcareous material showed porosity values as high as 7.2% whereas the specimens free from inclusions showed lower porosities. As shown in Figure 6 the porosities of unretorted specimens appear to decrease with increasing kerogen content. This trend is considered to be attributed to the inclusion of calcareous material which is commonly found in very lean Antrim oil shale. The porosities increase considerably after retorting. Figure 6 shows the change in porosity tends to increase proportionally to the percentage weight loss. Decrease in geometric density and increase in apparent density were also observed after retorting.

The permeabilities of unretorted specimens were extremely low, the highest value being in the order of 0.15 millidarcy. Permeabilities are higher in the bedding plane than in the perpendicular direction, but they were in the same order of magnitude (Figure 7). We found that retorting resulted in significant increases in permeability in both directions and the increase is relative to the percentage weight loss (Figure 8, 9). The amount of increase in the bedding direction after retorting was in two to three orders of magnitude as compared to unretorted specimens and in one to two orders of magnitude as compared to those in the perpendicular direction (Figure 10).

SEM micrographs enabled us to observe the pore structures of the retorted and unretorted specimens, thereby providing qualitative support to the measured data. Separation of bedding planes as well as loosening of grains is clearly exhibited in Figure 11. The magnification of the top portion of the micrograph is 1500X whereas the lower portion is 500X. Optical microscopy was also conducted to study the distribution of kerogen in retorted and unretorted specimens. It was found that the black kerogen present in the unretorted specimens disappeared or diminished in the case of retorted specimens.

DISCUSSION OF RESULTS

As described in the results, most of the specimens in general, and kerogen-rich specimens in particular, exhibited cracking and volumetric expansion. By the time the temperature reached 230°-290°C, many fractures parallel to the bedding plane were quite pronounced. This may be partly due to the inherent weakness of Antrim oil shale along the bedding plane. Inorganic cementation between some laminae was insufficient to overcome internal forces probably owing to the relief of internal stresses or pressure created by the vaporization of low molecular weight material (7). With further increase of temperature, existing fractures enlarged and additional ones developed. Once the fractures are formed the other factors, besides heating, that probably influenced their growth were swelling and formation of gases within the specimens. The kerogen-rich specimens experienced extensive structural breakdown by retorting which is due to the mechanically weak mineral matrix. The amount of fracturing and structural breakdown appeared to be a function of the organic content. The richer the oil shale, the greater the amount of fracturing and structural deformation. This type of structural response to heating of kerogen-rich specimens indicates that mineral constituents are loosely bound and the organic matter is predominant in the mineral matrix.

Pore space and fractures created during the retorting process result in significant decreases in strength and elastic modulus. The latter is ascribed to the crack closure and compaction. A significant reduction of Poisson's ratio displayed by the retorted specimens is considered to be attributed to the fact that the cracks are preferably orientated in the parallel direction to bedding, contributing to more axial deformation than to lateral deformation.

The volatilization of kerogen obviously increase porosity and permeability. The preferred orientation of the cracks, as evidenced in SEM microscopy, results in significantly higher permeability increase in the bedding plane. This property would be desirable for propagation of the combustion front in the horizontal direction.

Porosity and permeability are the most important factors governing the accumulation, migration and distribution of fluids in rocks. It has been shown in previous studies (9) that the effect of overburden pressure on porosity and permeability is significant enough to warrant consideration. In the present investigation of permeability, a radial stress field less than 1 MPa was applied through the rubber sleeve surrounding the specimen. But the porosity has been determined in the unconfined condition. In order to form more realistic concepts, we should measure porosity and permeability under simulated pressures existing at varying depths.

CONCLUSIONS

This study acquaints us with the changes in the mechanical and physical properties of Antrim oil shale on heating in air at 500°C in a stress free environment. It was observed that compressive strength, elastic modulus, and density decrease whereas maximum strain at failure increases on retorting. It was revealed that the permeability changes significantly on retorting both in the perpendicular and the parallel direction to bedding; one to two orders of magnitude increase in the parallel direction and two to three orders of magnitude in the perpendicular direction. The mechanical and physical properties appear to change in a predictable manner and are correlated with each other fairly well, at least qualitatively.

ACKNOWLEDGEMENT

The reported work was performed as a part of a subcontract to Dow Chemical Company under Department of Energy Contract No. EX-76-C-01-2346.

REFERENCES

(1) McGregor, D. J., "Stratigraphy of Upper Devonian and Mississipian Rocks in Michigan Basin", Bull. Am. Assoc. Petrol. Geologists, V. 38, No. 11, pp. 2324-2356.

(2) Matthews, R. D. and Humphrey, J. P., "A Search for Energy from the Antrim", SPE Paper 6494, Midwest Gas Storage and Production Symp., April 1977.

(3) Musser, W. N., "The Physical Properties and Chemical Composition of Antrim Oil Shale", Dow Chemical Co. Report FR310, Jan. 20, 1976, 91 p.

(4) Kim, K., "Mechanical Characteristics of Antrim Shale", DOE Open File Report FE-2346-24, 1978.

(5) Radcliffe, K. S. and Thill, R. E., "Bureau of Mines Oil Shale Bank", Proceedings of the 11th Oil Shale Symp., 1978.

(6) Tisot, P. R., "Alterations in Structure and Physical Properties of Green River Oil Shale by Thermal Treatment", J. of Chem. and Eng. Data, Vol. 12, No. 3, 1967.

(7) Tisot, P. R. and Sohns, H. W., "Structural Response of Rich Green River Oil Shale to Heat and Stress and its Relationship to Induced Permeability", J. of Chem. and Eng. Data, Vol. 15, No. 3, pp. 425-434, 1970.

(8) Mular, A. L., Hockings, W. A., and Fuerstenan, D. W., "A Simplified Air Pycnometer to Facilitate Powder Characterization", AIME Trans., Dec. 1963, pp. 404-406.

(9) Nelson, R. A., "An Experimental Study of Fracture Permeability in Porous Rock", Proceedings of 17th U.S. Symp. on Rock Mech., 1976.

(10) Singh, S. P., "A Laboratory Investigation on the Changes of Mechanical and Physical Properties of Michigan Oil Shale on Retorting", M.S. Thesis, Mining Engineering Dept., Michigan Technological University, 1979.

TABLE 1

Uniaxial Compression Test Results for Retorted and Unretorted Antrim Oil Shale Specimens (NX dia.)

Specimen No.	% Wt. Loss		Density (Mg/m^3)	Poisson's Ratio	Young's Modulus (GPa)	Compressive Strength (MPa)	Maximum Axial Strain (10^{-6})
101/1357.5	12.6	U*	2.360	0.13	13.04	105.57	9,750
		R+	2.069	0.03	1.02	34.47	39,500
101/1237.7	10.7	U	2.408	0.15	10.80	112.32	10,750
		R	2.151	0.04	2.40	55.09	30,375
101/1336.0	8.6	U	2.398	0.17	16.87	136.49	9,000
		R	2.186	0.07	3.46	83.17	25,750
101/1301.4	8.6	U	2.419	0.06	14.40	92.42	9,000
		R	2.205	0.02	2.10	50.48	30,500
102/1377.5	7.3	U	2.510	0.09	13.69	105.21	8,750
		R	2.327	0.07	2.23	54.03	31,000
101/1366.6	3.7	U	2.551	0.12	15.21	106.28	7,125
		R	2.457	0.07	13.86	96.50	9,250

*Unretorted specimen.

+Retorted specimen.

TABLE 2

Porosity, Permeability and Density of Unretorted and Retorted Specimens in Parallel and Perpendicular Directions to Bedding

Specimen No.		Parallel to Bedding				Perpendicular to Bedding			
		% Wt. Loss	Apparent Density (Mg/m^3)	Porosity (%)	Permeability (Millidarcies)	% Wt. Loss	Apparent Density (Mg/m^3)	Porosity (%)	Permeability (Millidarcies)
101/1332.3	U*	9.0	2.404	1.9	0.035	9.4	2.389	0.8	0.020
	R+		2.762	25.5	15.430		2.758	23.8	0.116
101/1333.3	U	6.9	2.492	2.2	0.032	7.3	2.461	0.9	0.017
	R		2.654	15.0	5.051		2.678	16.8	0.098
101/1347.9	U	8.0	2.403	-	0.029	7.4	2.420	0.2	0.021
	R		2.731	19.6	10.306		2.729	19.8	0.141
101/1350.1	U	3.7	2.429	0.6	0.025	6.2	2.482	3.4	0.004
	R		2.728	15.4	2.554		2.717	18.4	0.077
101/1359.9	U	11.8	2.366	1.9	0.027	8.2	2.433	1.9	0.021
	R		2.778	27.3	15.244		2.760	21.6	0.101
101/1368.6	U	5.2	2.519	4.4	0.032	5.2	2.508	4.3	0.029
	R		2.719	16.7	1.608		2.708	16.7	0.082
101/1412.3	U	4.5	2.504	1.1	0.123	2.7	2.578	5.2	0.024
	R		2.697	13.4	2.823		2.707	12.4	0.072
102/1257.3	U	10.6	2.294	1.9	0.046	11.4	2.289	1.7	0.044
	R		2.692	26.9	7.660		2.740	27.0	0.122
102/1415.9	U	4.4	2.472	1.9	0.032	3.0	2.588	5.2	0.027
	R		2.762	16.4	1.718		2.702	12.3	0.064
101/1511.4	U	1.0	2.740	7.2	0.085	1.0	2.740	7.2	0.041
	R		2.746	9.2	1.358		-	-	-

*Unretorted specimen.

+Retorted specimen.

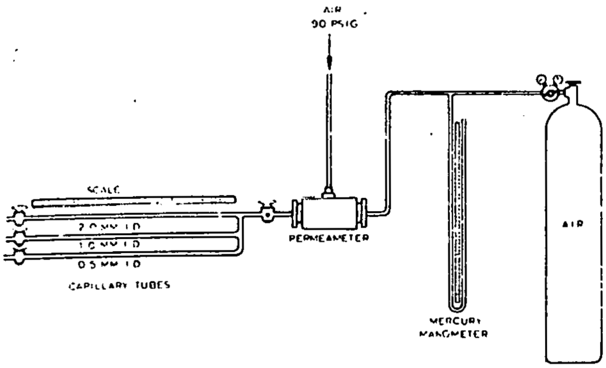

Fig. 1 - Schematic diagram of permeability measurement apparatus.

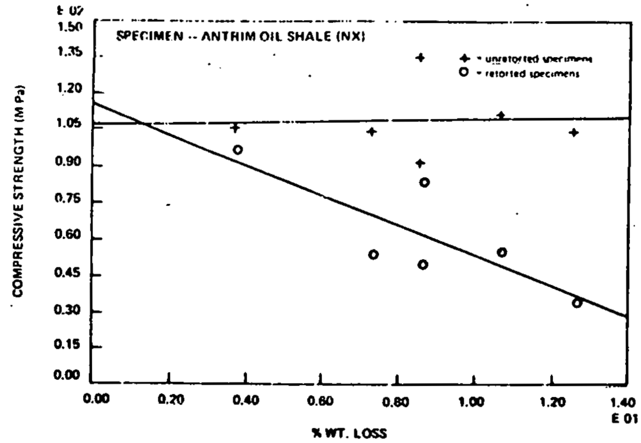

Fig. 2 - Compressive strength of unretorted and retorted specimens vs. kerogen content.

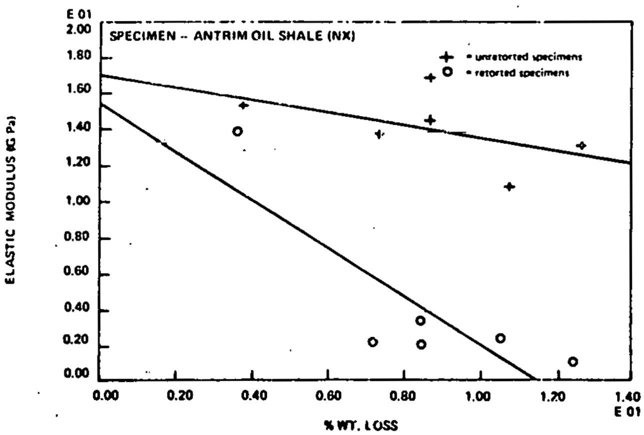

Fig. 3 - Elastic modulus of unretorted and retorted specimens vs. kerogen content.

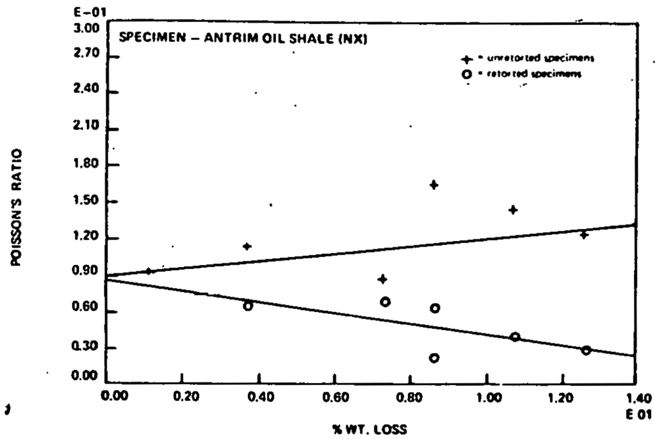

Fig. 4 - Poisson's ratio of unretorted and retorted specimens vs. kerogen content.

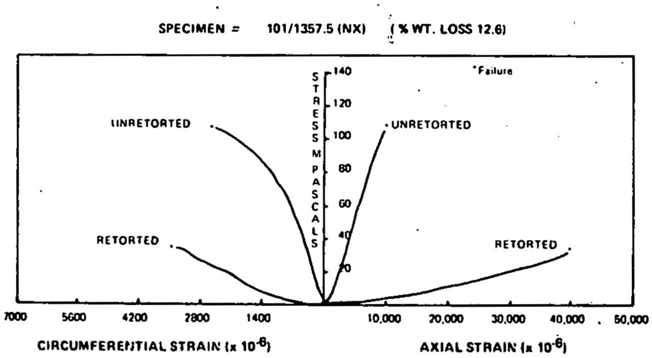

Fig. 5 - Typical stress-strain curves of unretorted and retorted specimens.

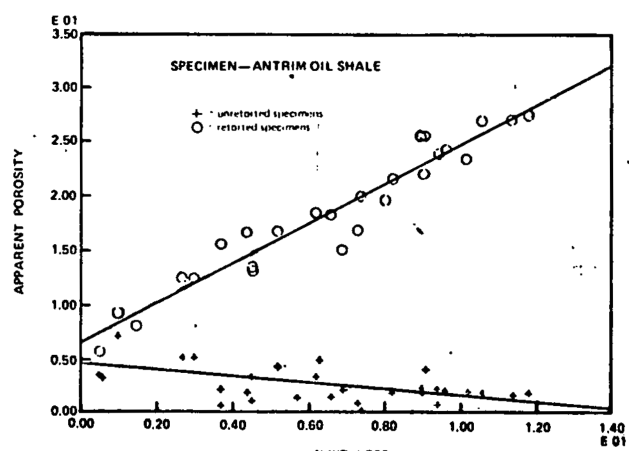

Fig. 6 - Apparent porosity of unretorted and retorted specimens vs. kerogen content.

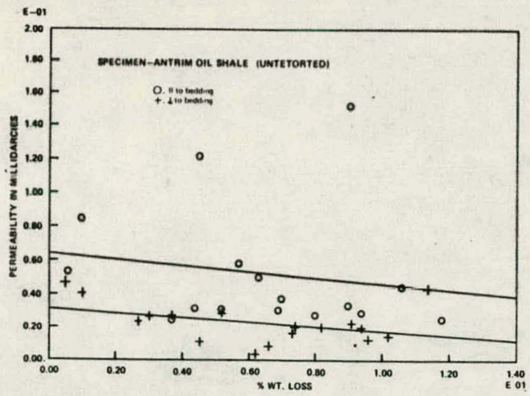

Fig. 7 - Permeability of unretorted specimens vs. kerogen content.

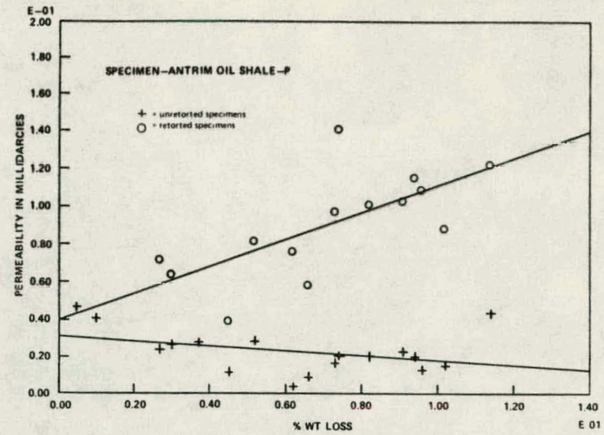

Fig. 8 - Permeability of unretorted and retorted specimens cored from perpendicular direction to bedding vs. kerogen content.

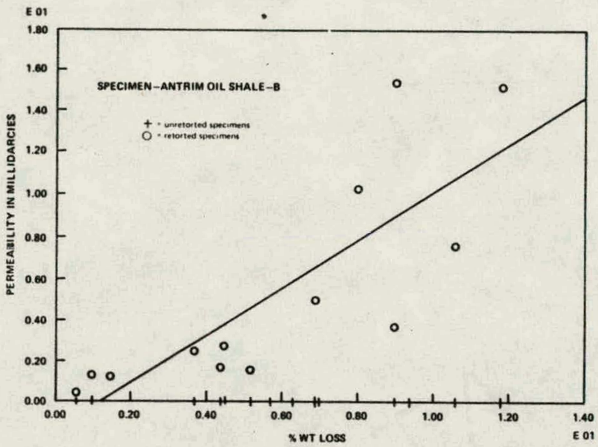

Fig. 9 - Permeability of unretorted and retorted specimens cored from parallel direction to bedding vs. kerogen content.

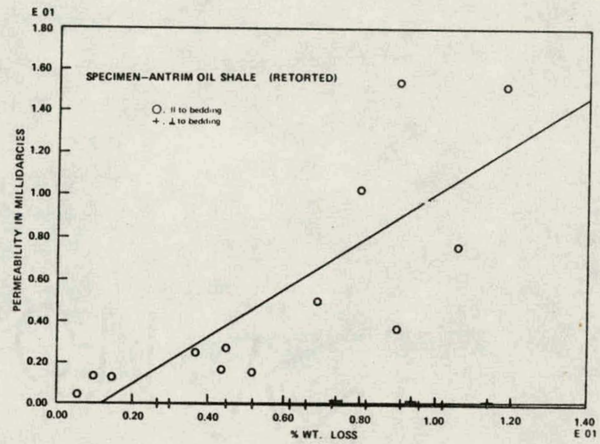

Fig. 10 - Permeability of retorted specimens vs. kerogen content.

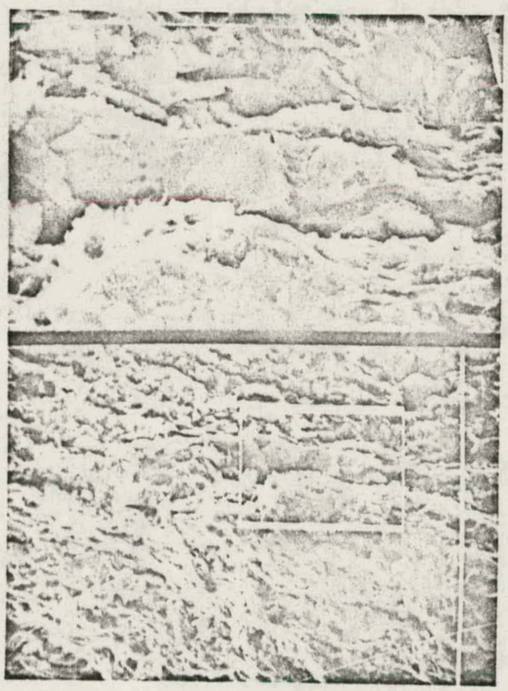

Fig. 11 - Scanning electron micrograph of a fractured surface of retorted specimen.